

Stoichiometric Dependence on Structural and Electronic Properties of $\text{HfX}_{2(1-x)}\text{X}_{2x}$ ($\text{X}=\text{S}, \text{Se}, \text{Te}$) monolayers[†]

Vivek Mahajan^{1*}, and Hitesh Sharma^{1,2}

¹*Department of Physics, I.K. G Punjab Technical University, Kapurthala,
Punjab, India*

²*National Institute of Technology, Delhi, India*

E-mail: vivekk.mahajann@gmail.com, and hitesh@ptu.ac.in

Supporting Information Available

Calculating phonon frequencies of HfX_2 .

In this section, the phonon frequency of HfX_2 monolayers has been calculated, and atom-wise numbering on the supercell is shown.

The above plot shows that HfS_2 and HfSe_2 monolayers are thermally stable, whereas HfTe_2 is unstable due to the presence of negative imaginary frequencies.

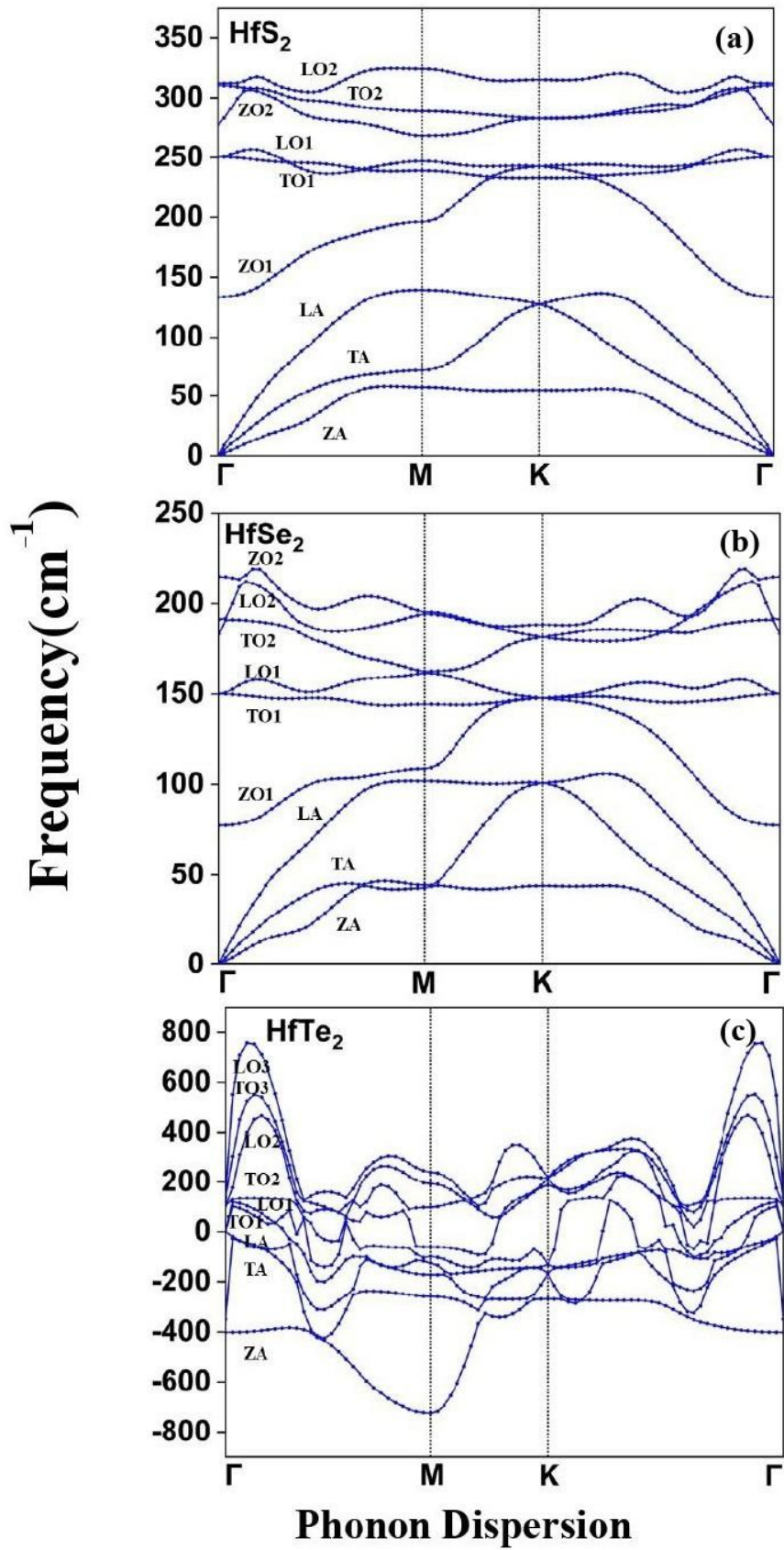


Figure S1: Phonon dispersion plot of HfX₂ (X=S, Se, Te) monolayers.

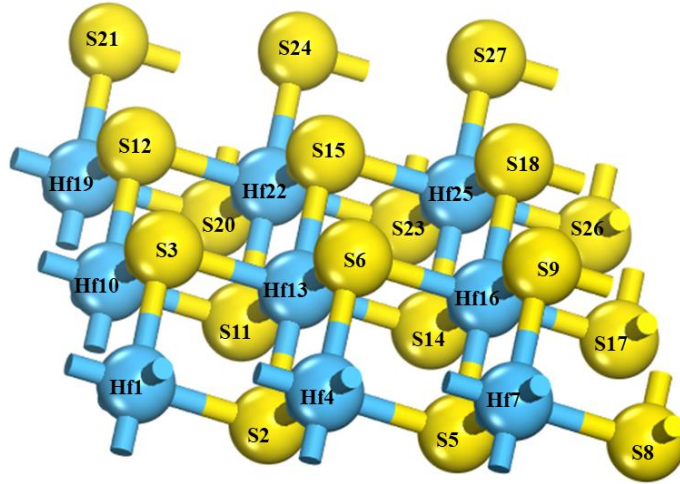


Figure S2: Atom-wise numbering on $\text{HfX}_{2(1-x)}\text{X}_{2x}$ ($X=\text{S, Se, Te}$) systems.

Effect of SOC in Hf-alloy.

In this section, the tabular data of Hf-alloy are compared with the PBE and PBE+SOC functional. Also, the relativistic effect has been investigated at the Γ point.

Table S1: Tabular data of the calculated electronic band gap of $\text{HfX}_{2(1-x)}\text{X}_{2x}$ ($X=\text{S, Se, Te}$) systems by making a comparison between the PBE and PBE+SOC functional.

S. No	Number of doped atoms	Calculated E_{gap} (eV)			
		For HfS_2			
		With Se doping		With Te doping	
		PBE	PBE+SOC	PBE	PBE+SOC
1.	Pure	1.26	1.26	1.26	1.26
2.	2	1.11	1.11	0.65	0.65
3.	4	0.98	0.98	0.45	0.45
4.	6	0.84	0.84	0.00	0.00
5.	8	0.77	0.77	0.00	0.00
		For HfSe_2			
		With S doping		With Te doping	
		PBE	PBE+SOC	PBE	PBE+SOC
1.	Pure	0.55	0.55	0.55	0.55
2.	2	0.51	0.51	0.24	0.24
3.	4	0.57	0.57	0.12	0.12
4.	6	0.73	0.73	0.00	0.00
5.	8	0.70	0.70	0.00	0.00
		For HfTe_2			
		With S doping		With Te doping	
		PBE	PBE+SOC	PBE	PBE+SOC

1.	Pure	0.00	0.00	0.00	0.00
2.	2	0.00	0.00	0.00	0.00
3.	4	0.00	0.00	0.00	0.00
4.	6	0.00	0.00	0.00	0.00
5.	8	0.00	0.00	0.00	0.00

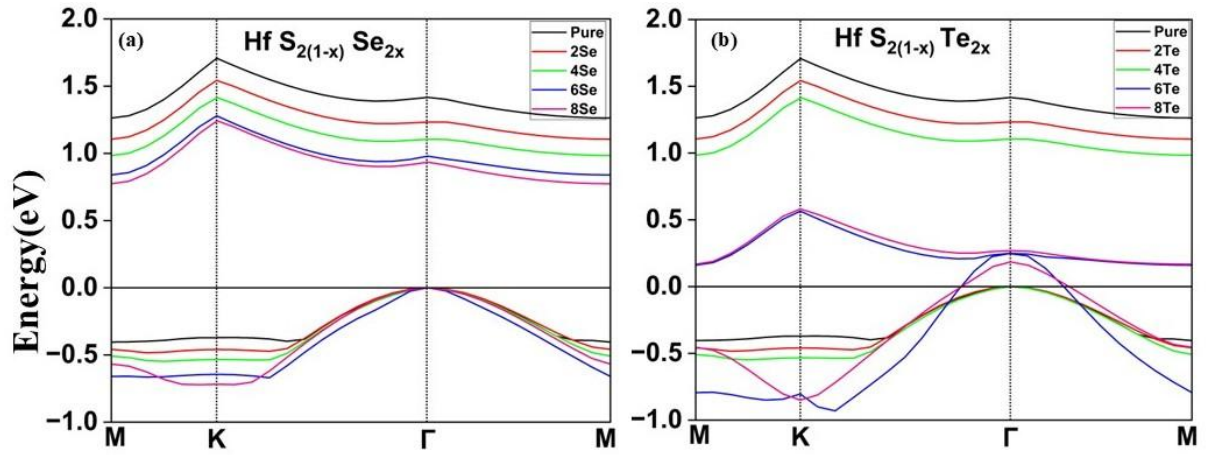


Figure S3: (a) and (b) show the electronic band structure plots of $\text{HfS}_{2(1-x)}\text{Se}_{2x}$, and $\text{HfS}_{2(1-x)}\text{Te}_{2x}$ systems with varied doping atom concentrations using the PBE+SOC functional at the Γ point.

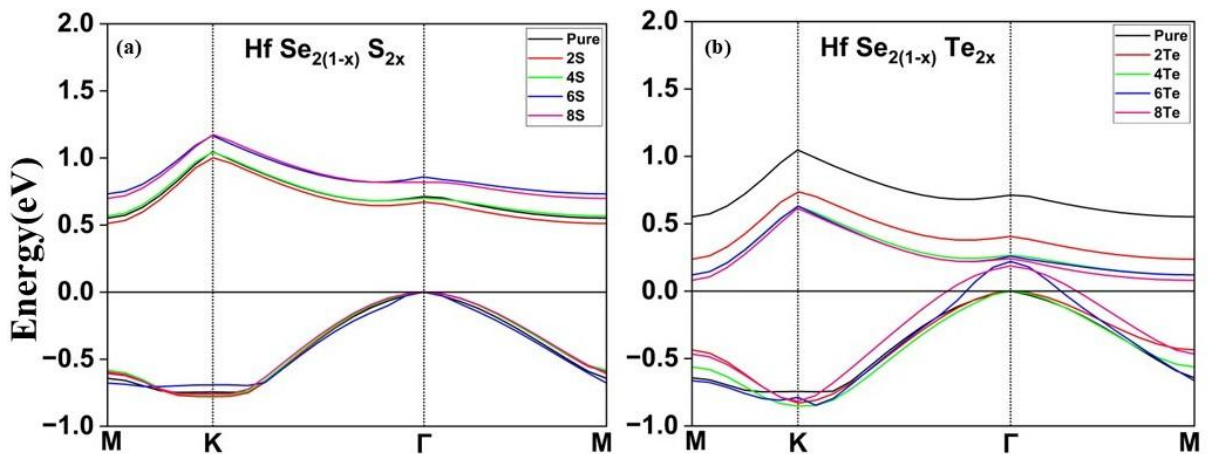


Figure S4: (a) and (b) show the electronic band structure plots of $\text{HfSe}_{2(1-x)}\text{S}_{2x}$, and $\text{HfSe}_{2(1-x)}\text{Te}_{2x}$ systems with varied doping atom concentrations using the PBE+SOC functional at the Γ point.

Tabular data of the effective mass of Hf-alloy

Table S2: Effective mass (m^*) of HfS₂, doped HfS_{2(1-x)}Se_{2x} and HfSe_{2(1-x)}S_{2x}, and HfSe₂ systems.

S. No	S	Se	Effective Mass (m^*)	
			m_e	m_h
1	1	0	-0.02	0.02
2	0.89	0.11	-0.02	0.02
3	0.78	0.22	-0.02	0.02
4	0.67	0.33	-0.02	0.02
5	0.56	0.44	-0.02	0.02
6	0.44	0.56	-0.02	0.02
7	0.33	0.67	-0.02	0.02
8	0.22	0.78	-0.02	0.03
9	0.11	0.89	-0.02	0.01
10	0	1	-0.02	0.01

Table S3: Effective mass (m^*) of HfS₂, doped HfS_{2(1-x)}Te_{2x} and HfTe_{2(1-x)}S_{2x}, and HfTe₂ systems.

S. No	S	Te	Effective Mass (m^*)	
			m_e	m_h
1	1	0	-0.02	0.02
2	0.89	0.11	-0.04	0.02
3	0.78	0.22	-0.02	0.02
4	0.67	0.33	-0.01	0.01
5	0.56	0.44	-0.02	0.04
6	0.44	0.56	-0.03	0.02
7	0.33	0.67	-0.03	0.04
8	0.22	0.78	-0.02	0.04
9	0.11	0.89	-0.02	0.04
10	0	1	-0.02	0.02

Table S4: Effective mass (m^*) of HfSe₂, doped HfSe_{2(1-x)}S_{2x} and HfTe_{2(1-x)}Se_{2x}, and HfTe₂ systems.

S. No	Se	Te	Effective Mass (m^*)	
			m_e	m_h
1	1	0	-0.02	0.01
2	0.89	0.11	-0.01	0.02
3	0.78	0.22	-0.01	0.02
4	0.67	0.33	-0.03	0.02
5	0.56	0.44	-0.02	0.02
6	0.44	0.56	-0.02	0.02
7	0.33	0.67	-0.02	0.02
8	0.22	0.78	-0.02	0.02
9	0.11	0.89	-0.03	0.04
10	0	1	-0.02	0.02